

## Single-crystal Raman Study of Some Aquo-pentachloro-salts $[\text{MCl}_5(\text{H}_2\text{O})]^{2-}$ (M = In or Fe)

By D. M. Adams\* and D. C. Newton, Department of Chemistry, University of Leicester, Leicester LE1 7RH

Raman single-crystal spectra are reported for eight hydrates and deuteriates  $[\text{MCl}_5(\text{H}_2\text{O})]^{2-}$  (M = In or Fe). Many fewer lattice modes were found than predicted, but for the anion internal modes factor-group predictions accord well with observation. A complete assignment in terms of anion  $C_{4v}$  symmetry is deduced. Deuteriation enabled identification of all skeletal modes associated with oxygen-atom motions. The most unusual feature of the assignments is that  $\pi(\text{MCl}_4)$  modes come above  $\delta(\text{MCl}_4)$  modes. Comparison with single-crystal assignments for  $[\text{InCl}_5]^{2-}$  show that the largest change is in the  $A_1 \pi(\text{InCl}_4)$  mode which is raised upon aquation of the complex.

IN earlier work on the i.r. and Raman spectra of the series  $[\text{FeCl}_5(\text{H}_2\text{O})]^{2-}$  and  $[\text{InCl}_5(\text{H}_2\text{O})]^{2-}$  it was found that powder samples yielded spectra which had considerably fewer bands than predicted.<sup>1</sup> This was taken to mean that many closely spaced bands overlapped. It was difficult to suggest more than outline assignments based upon general appreciation of ranges in which particular vibrations occur. In this paper we report the results of several Raman single-crystal studies on compounds of this type. These results are a considerable improvement upon the powder work and allow an assignment to be made for all the internal modes of the anions.

The  $\text{K}^+$  and  $\text{NH}_4^+$  salts of  $[\text{FeCl}_5(\text{H}_2\text{O})]^{2-}$ , and  $(\text{NH}_4)_2[\text{InCl}_5(\text{H}_2\text{O})]$  are isomorphous.<sup>2</sup> They have the symmetry  $Pnma$  ( $D_{2h}^{10}$ ) with  $z = 4$ . Each metal atom is in approximately octahedral co-ordination; the octahedra are so arranged in the unit cell that the  $\text{M} \leftarrow \text{OH}_2$  bonds are all in the  $ac$  plane (see Figure 1). All the compounds used in this study are believed to adopt the same structure.

### EXPERIMENTAL

Crystals of the compounds  $\text{M}^I_2[\text{FeCl}_5(\text{H}_2\text{O})]$  were grown by slow evaporation of aqueous solutions of  $\text{FeCl}_3 \cdot 6\text{H}_2\text{O}$  and the appropriate salt,  $\text{KCl}$ , etc.  $\text{Cs}_2[\text{InCl}_5(\text{H}_2\text{O})]$  crystals were obtained by slow evaporation of aqueous

solutions of  $\text{CsCl}$  and hydrated indium trichloride. We were unable to grow suitable crystals of the ammonium salt.

Corresponding deuteriates were obtained by evaporation

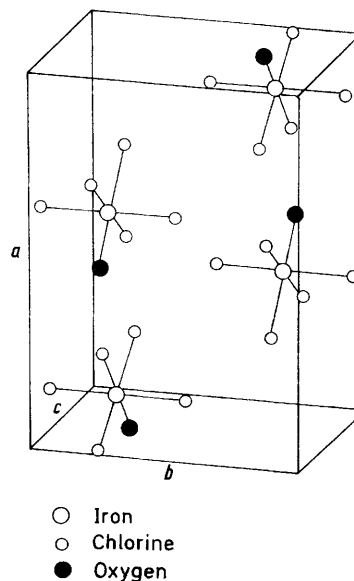


FIGURE 1 Anion positions in the unit cell of  $\text{K}_2[\text{FeCl}_5(\text{H}_2\text{O})]$

of solutions of the appropriate anhydrous salts over dried silica gel.  $(\text{ND}_4)_2[\text{FeCl}_5(\text{D}_2\text{O})]$  was crystallised from a solution of  $\text{NH}_4\text{Cl}$  and  $\text{FeCl}_3$  in a large excess of  $\text{D}_2\text{O}$ .

\* D. M. Adams and P. J. Lock, *J. Chem. Soc. (A)*, 1971, 2801.

<sup>2</sup> R. W. G. Wyckoff, 'Crystal Structures,' 2nd edn., vol. 3, Interscience, New York, 1965.

TABLE 1  
Factor-group analysis for  $K_2FeCl_5(H_2O)^a$

$D_{2h}$	$A_g$	$B_{1g}$	$B_{2g}$	$B_{3g}$	$A_u$	$B_{1u}$	$B_{2u}$	$B_{3u}$
$N_T$	16	11	16	11	11	16	11	16
$T_A$						1	1	1
$T$	5	4	5	4	4	4	3	4
$R$	1	2	1	2	2	1	2	1
$N_i$	10	5	10	5	5	10	5	10

## Activities

	Raman				I.r.		
	$xx$	$xy$	$zx$	$yz$	$z$	$y$	$x$
$yy$							
$zz$							

Internal co-ordinates								
$\nu(Fe-OH_2)$	1	0	1	0	0	1	0	1
$\nu(Fe-Cl)$	4	1	4	1	1	4	1	4

<sup>a</sup> Hydrogen atoms are ignored.  $N_T$  = Total number of modes of unit cell;  $T_A$  = acoustic modes;  $T$  = translatory lattice modes;  $R$  = rotatory lattice modes;  $N_i$  = number of internal modes.

TABLE 2  
Observed Raman frequencies ( $cm^{-1}$ ) and peak heights (arbitrary units) for crystals of  $Cs_2[InCl_5(H_2O)]$  at ambient temperature

$\Delta/cm^{-1}$	$z(xx)y$	$x(yy)z$	$x(zz)y$	$x(zy)z$	$x(zx)z$	$x(yx)z$	$D_{2h}$
44						10	$B_{1g}$
48				11			$B_{3g}$
52			11				$A_g$
66	30	22	13				$A_g$
76				16			$B_{3g}$
90	21		4				$A_g$
124				7		27	$B_{1g}$
149		20		10			$A_g + B_{3g}$
162	185	15	55	40	7	142	$A_g + B_{1g} + B_{2g}$
174				26			$B_{3g}$
178						77	$B_{1g}$
184	26	25					$A_g$
190					6		$B_{2g}$
215		6	6				$A_g$
256						8	$B_{1g}$
271	250	106	46				$A_g$
280	60	98	49				$A_g$
310	60	167	23		6		$A_g$

TABLE 4

Observed Raman frequencies ( $cm^{-1}$ ) and peak heights (arbitrary units) for crystals of  $K_2[FeCl_5(H_2O)]$  at ambient temperature

$\Delta/cm^{-1}$	$z(xx)y$	$z(xy)y$	$x(yy)z$	$x(zy)z$	$x(zx)y$	$x(yx)y$	$x(zz)y$	$x(yz)y$	$D_{2h}$
38		6				4	32		$A_g$
47	240	14			39	9	25		$A_g + B_{2g}$
70							50	6	$A_g$
77	43				16	39			$B_{1g} + B_{2g}$
85	18						16	6	$A_g$
89					58				$B_{3g}$
124	32						19		$A_g$
129						69			$B_{1g}$
132			76					44	$B_{3g}$
174					43	6		66	$B_{3g}$
177			130						$B_{1g}$
180					48				$B_{3g}$
183	168						75		$A_g$
190	139						89		$A_g$
222		67			48			48	$B_{1g} + B_{3g}$
226	52					56			$A_g + B_{2g}$
276		5		38			89		$A_g + B_{1g}$
300	252	74	5	6		6	4		$A_g$
384	52	7	250	14	14	59	240	23	$A_g$
			51			6	35	2	$A_g$

The absence of O-H was checked by examination of the stretching region. Composition was checked by halogen analysis.

The crystals grown all had similar morphology, showing principally the faces of a distorted octahedron. The position of the axes was established from Weissenberg

TABLE 3

Observed Raman frequencies ( $cm^{-1}$ ) and peak heights (arbitrary units) for crystals of  $Cs_2[InCl_5(D_2O)]$  at ambient temperature

$\Delta/cm^{-1}$	$x(yy)z$	$x(zy)z$	$y(zz)x$	$y(zy)x$	$y(xz)x$	$y(xy)x$	$D_{2h}$
36	14	7		15			$A_g + B_{3g}$
50	11	23	11	58			$A_g + B_{3g}$
66	14	4	36				$A_g$
90			16				$A_g$
126		17		35		18	$B_{1g} + B_{3g}$
148	19	32		64			$A_g + B_{3g}$
160			160		11	130	$A_g + B_{1g}$
168	19	100		193			$B_{3g}$
174						56	$B_{1g}$
186	24						$A_g$
191					8		$B_{2g}$
213			11				$A_g$
270	64		110	9		11	$A_g$
282	10		113	12			$A_g$
300	176		211	10		9	$A_g$

X-ray diffraction photographs of a small crystal of  $(NH_4)_2[FeCl_5(H_2O)]$ . In addition to octahedral faces the crystals exhibited (100) faces which were set normal to the propagation of the light in many experiments. For other runs faces were ground and polished normal to the  $b$  and  $c$  axes.

Raman spectra were obtained with a Coderg PH1 spectrometer with 632.8 nm excitation (ca. 35 mW at the sample). Cooling the crystals to ca. 120 K revealed no feature not present at room temperature.

## RESULTS AND ASSIGNMENT

The results from the eight single crystals used are in Tables 2—9. They show a high degree of consistency. Taken together (Table 10) it is seen that some spectra show more bands than others owing to individual variations

TABLE 5

Observed Raman frequencies ( $\text{cm}^{-1}$ ) and peak heights (arbitrary units) for crystals of  $\text{K}_2[\text{FeCl}_5(\text{D}_2\text{O})]$  at ambient temperature

$\Delta/\text{cm}^{-1}$	$x(yy)z$	$x(z)y$	$x(zx)z$	$x(yx)z$	$x(zz)y$	$x(yz)y$	$D_{2h}$
48			18				$B_{2g}$
73					38		$A_g$
78				22			$B_{1g}$
86					4		$A_g$
90			27				$B_{2g}$
124					15		$A_g$
129				39			$B_{1g}$
133						25	$B_{3g}$
179	5	29				46	$B_{3g}$
190			9		82		$A_g$
215		20		31		33	$B_{1g} + B_{3g}$
225	18		10		57		$A_g + B_{2g}$
300	173	9	20	20	210	34	$A_g$
371	31		4		28	5	$A$

TABLE 6

Observed Raman frequencies ( $\text{cm}^{-1}$ ) and peak heights (arbitrary units) for crystals of  $\text{Rb}_2[\text{FeCl}_5(\text{H}_2\text{O})]$  at ambient temperature

$\Delta/\text{cm}^{-1}$	$x(yy)z$	$x(z)y$	$x(zx)z$	$x(yx)z$	$x(zz)y$	$x(yz)y$	$D_{2h}$
41			10				$B_{2g}$
65			9		42		$A_g + B_{2g}$
73			12		5		$B_{2g}$
94				23		6	$B_{1g}$
133				28	9		$B_{1g}$
136		13				21	$B_{3g}$
180	6	28		64	5	44	$B_{1g} + B_{3g}$
189			11		76		$A_g$
210		15		28		24	$B_{1g} + B_{3g}$
218	12		5		36		$A_g + B_{2g}$
272	7			4			$A_g + B_{1g}$
296	183	8	22	22	185	20	$A_g$
350	26		3		24		$A_g$

TABLE 8

Observed Raman frequencies ( $\text{cm}^{-1}$ ) and peak heights (arbitrary units) for crystals of  $(\text{ND}_4)_2[\text{FeCl}_5(\text{D}_2\text{O})]$  at ambient temperature

$\Delta/\text{cm}^{-1}$	$z(xx)y$	$z(yx)y$	$z(yy)x$	$z(yx)x$	$x(zz)y$	$x(yz)y$	$x(zx)y$	$x(yx)y$	$D_{2h}$
34	6								$A_g$
46								18	$B_{2g}$
50	200	3		4					$A_g$
70					31		21		$A_g + B_{2g}$
81		12		10				22	$B_{1g}$
113			4						$A_g$
119	7						24		$A_g + B_{2g}$
126		18		21		10		32	$B_{1g}$
146						10			$B_{3g}$
184		28		24		35	45	71	$B_{1g} + B_{2g} + B_{3g}$
194	82				60		47		$A_g + B_{2g}$
200		30		27		42		72	$B_{1g} + B_{3g}$
210			12		25				$A_g$
269				3				4	$B_{1g}$
297	171	7	181	9	164	30	88	74	$A_g$
340	20		30		27	6	15	16	$A_g$

of intensity, but the pattern of behaviour is clear from the whole set. The spectra apparently show one third to one half the number of bands predicted by factor-group analysis<sup>3</sup> (Table 1).

<sup>3</sup> D. M. Adams and D. C. Newton, 'Tables for Factor Group and Point Group Analysis,' Beckman-RIIC Limited, Croydon, 1970; D. M. Adams and D. C. Newton, *J. Chem. Soc. (A)*, 1970, 2282.

Since these are all chloro-complexes we can be quite sure (from comparison with simpler species) that none of the internal modes will lie below  $100 \text{ cm}^{-1}$ . We can be equally confident that for the  $\text{K}^+$ ,  $\text{Rb}^+$ , and  $\text{Cs}^+$  salts at least, none of the lattice modes will be much above  $100 \text{ cm}^{-1}$ . The spectra confirm this belief, showing a clear gap of  $34 \text{ cm}^{-1}$

TABLE 7

Observed Raman frequencies ( $\text{cm}^{-1}$ ) and peak heights (arbitrary units) for crystals of  $(\text{NH}_4)_2[\text{FeCl}_5(\text{H}_2\text{O})]$  at ambient temperature

$\Delta/\text{cm}^{-1}$	$x(yy)z$	$x(z)y$	$x(zx)z$	$x(yx)z$	$x(zz)y$	$x(yz)y$	$D_{2h}$
34	7				30		$A_g$
46				14			$B_{2g}$
50					16		$A_g$
71			6		42		$A_g$
82		5		30			$B_{1g}$
112	6						$A_g$
118		13	5		23	5	$A_g + B_{2g} + B_{3g}$
128				38			$B_{1g}$
138			10				$B_{2g}$
184		30				17	$B_{3g}$
187				44			$B_{1g}$
194					52		$A_g$
210		31		53		19	$B_{1g} + B_{3g}$
218	12				27		$A_g$
296	181		9	3	178	5	$A_g$
353	27				27		$A_g$

or more in the expected region. For the ammonium salts lattice modes will most probably rise above  $100 \text{ cm}^{-1}$ , and there is the additional complication that cation rotatory modes are allowed, although we have found no evidence of them.

For a single anion  $[\text{MCl}_5(\text{H}_2\text{O})]^{2-}$  of  $C_{4v}$  symmetry 11 internal modes are predicted; all are Raman-active.

Their approximate forms are listed in Table 11, and correlated to factor-group symmetry species *via* the site group.

Factor-group analysis shows that each  $A_g$  mode should be accompanied by a  $B_{2g}$  mode and, similarly, that  $B_{1g}$  and  $B_{3g}$  modes should be equal in number. Two significant facts are immediately apparent: (i) There is a substantial deficit of lattice modes. The greatest number found is for  $\text{K}_2[\text{FeCl}_5(\text{H}_2\text{O})]$  which shows only 7 of the predicted 24!

However, this is the least interesting spectral region for our purpose as we are most concerned with the anion internal modes. The generally higher lattice modes found

vanishingly low intensities of these modes. Figure 2 shows how a set of four vectors along the  $C_{4v}$  principal

TABLE 9

Observed Raman frequencies ( $\text{cm}^{-1}$ ) and peak heights (arbitrary units) for crystals of  $\text{Cs}_2[\text{FeCl}_5(\text{H}_2\text{O})]$  at ambient temperature

$\Delta/\text{cm}^{-1}$	$x(yy)z$	$x(zy)z$	$x(zx)z$	$x(yx)z$	$x(zz)y$	$x(yz)y$	$D_{2h}$
37	6		6	75		4	$B_{1g}$
46			11				$B_{2g}$
53	14						$A_g$
57		8		15		8	$B_{1g} + B_{3g}$
63			9				$B_{2g}$
87				15			$B_{1g}$
115		4	24				$B_{2g}$
127	7			81		4	$B_{1g}$
167	53	11	92		49	4	$A_g + B_{2g}$
177				43	8		$B_{1g}$
224				8	12		$A_g + B_{1g}$
250			10				$B_{2g}$
278				8			$B_{1g}$
312	167	25	22	21	172	14	$A_g$

for the  $\text{NH}_4^+$  and  $\text{ND}_4^+$  salts strongly suggest that these modes are associated with translations of the cations.

(ii) A count of internal modes under  $D_{2h}$  symmetry

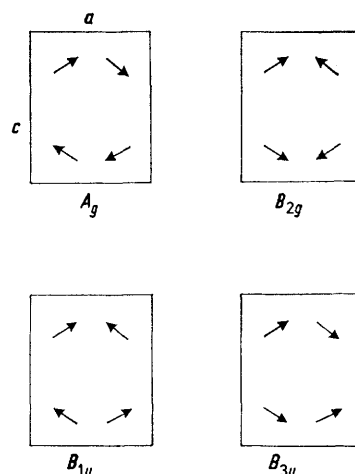


FIGURE 2 Coupling of four oriented vectors in the  $D_{2h}^{16}$  unit cell

axes of the anions couple (projected onto the crystallographic  $ac$  plane). It is seen that the motions associated with the

TABLE 10

Raman frequencies and principal symmetry species for the compounds  $\text{M}^{\text{I}}_2\text{M}^{\text{III}}\text{Cl}_5(\text{H}_2\text{O})$

$\text{Cs}_2\text{InCl}_5\text{-}(\text{H}_2\text{O})$	$\text{Cs}_2\text{InCl}_5\text{-}(\text{D}_2\text{O})$	$\text{K}_2\text{FeCl}_5\text{-}(\text{H}_2\text{O})$	$\text{K}_2\text{FeCl}_5\text{-}(\text{D}_2\text{O})$	$\text{Rb}_2\text{FeCl}_5\text{-}(\text{H}_2\text{O})$	$(\text{NH}_4)_2\text{FeCl}_5\text{-}(\text{H}_2\text{O})$	$(\text{ND}_4)_2\text{FeCl}_5\text{-}(\text{D}_2\text{O})$	$\text{Cs}_2\text{FeCl}_5\text{-}(\text{H}_2\text{O})$
44 $B_{1g}$	36 $A_g^* + B_{3g}$	38 $A_g$			34 $A_g$	34 $A_g$	37 $B_{1g}$
48 $B_{3g}$	50 $A_g^* + B_{3g}$	47 $A_g + B_{2g}$	48 $B_{2g}$	41 $B_{2g}$	46 $B_{2g}$	46 $B_{2g}$	46 $B_{2g}$
52 $A_g$					50 $A_g$	50 $A_g$	53 $A_g^*$
66 $A_g^*$	66 $A_g^*$						57 $B_{1g} + B_{3g}$
76 $B_{3g}$		70 $A_g$	73 $A_g$	65 $A_g$	71 $A_g + B_{2g}$	70 $A_g + B_{2g}$	63 $B_{2g}$
90 $A_g$	90 $A_g$	77 $B_{1g}$	78 $B_{1g}$		82 $B_{1g}$	81 $B_{1g}$	87 $B_{1g}$
		85 $A_g$	86 $A_g$		112 $A_g^*$	113 $A_g^*$	
		89 $B_{2g}$	90 $B_{2g}$	73 $B_{2g}$	118 $A_g + B_{2g}$	119 $A_g + B_{2g}$	115 $B_{2g}$
				94 $B_{1g}$			
124 $B_{1g} + B_{3g}$	126 $B_{1g} + B_{3g}$	124 $A_g$	124 $A_g$				
		129 $B_{1g}$	129 $B_{1g}$	133 $B_{1g}$	128 $B_{1g}$	126 $B_{1g}$	127 $B_{1g}$
		132 $B_{3g}$	133 $B_{3g}$	136 $B_{3g}$	138 $B_{2g}$		
149 $A_g^* + B_{3g}$	148 $A_g^* + B_{3g}$	174 $B_{3g}$				146 $B_{3g}$	
		177 $B_{1g}$					
162 $A_g + B_{1g} + B_{3g}$	160 $A_g + B_{1g}$	180 $B_{3g}$	179 $B_{3g}$	180 $B_{1g} + B_{3g}$	184 $B_{3g}$	184 $B_{1g} + B_{3g}$	177 $B_{1g}$
		183 $A_g$			187 $B_{1g}$		
174 $B_{3g}$	168 $B_{3g}$						
178 $B_{1g}$	174 $B_{1g}$	222 $B_{1g} + B_{3g}$	215 $B_{1g} + B_{3g}$	210 $B_{1g} + B_{3g}$	210 $B_{1g} + B_{3g}$	200 $B_{1g} + B_{3g}$	224 $A_g + B_{1g}$
184 $A_g^*$	186 $A_g^*$	190 $A_g$	190 $A_g$	189 $A_g$	194 $A_g$	194 $A_g + B_{2g}$	167 $A_g^* + B_{2g}$
190 $B_{2g}$	191 $B_{2g}$						
215 $A_g^*$	213 $A_g$	226 $A_g^* + B_{2g}$	225 $A_g^* + B_{2g}$	218 $A_g^* + B_{2g}$	218 $A_g^*$	210 $A_g^*$	
256 $B_{1g}$		276 $A_g^* + B_{1g}$		272 $A_g^* + B_{1g}$		269 $B_{1g}$	
271 $A_g^*$	270 $A_g^*$						
280 $A_g^*$	282 $A_g^*$	300 $A_g^*$	300 $A_g^*$	296 $A_g^*$	296 $A_g^*$	297 $A_g^*$	278 $B_{1g}$
310 $A_g^*$	300 $A_g^*$	384 $A_g^*$	371 $A_g^*$	350 $A_g^*$	353 $A_g^*$	340 $A_g^*$	250 $B_{2g}$
							312 $A_g^*$

Frequencies in  $\Delta \text{cm}^{-1}$ . \* Indicates a non-zero  $yy$  component.

(taking only  $\text{K}^+$ ,  $\text{Rb}^+$ , and  $\text{Cs}^+$  salts to avoid the complication of  $\text{NH}_4^+$  modes) (Table 12) shows that whilst  $B_{1g}$  and  $B_{3g}$  modes occur in roughly equal numbers, there is a pronounced shortage of  $B_{2g}$  modes. This is so marked as to point to a general mechanism responsible for the

$B_{2g}$  mode are largely self-cancelling and can be expected to be associated with very small changes in polarisability.

Taking  $\text{K}_2[\text{FeCl}_5(\text{H}_2\text{O})]$  as typical of the series we consider its spectrum in detail.

$B_2$  and  $E$  Modes.—Seven of the predicted 10  $A_g/B_{2g}$

modes and 4 of the expected 5  $B_{1g}/B_{3g}$  modes are found. Closer examination shows that each  $B_{1g}$  is accompanied by a  $B_{3g}$  band which is either close to or coincident with it, except for the 180 ( $B_{3g}$ ) and 276  $\text{cm}^{-1}$  ( $B_{1g}$ ) bands. However,

TABLE 11

Anion symmetry	Site symmetry	Factor group ( $4$ anions)
$C_{4v}$	$C_s$	$D_{2h}$
$\nu_1 \nu(\text{M} \leftarrow \text{OH}_2)$	$A_1$ $B_1$ $B_2$ $E$	$A' \xrightarrow{\times 4} A_g + B_{2g} + B_{1u} + B_{3u}$ $A'' \xrightarrow{\times 4} B_{1g} + B_{3g} + A_u + B_{2u}$
$\nu_2 \nu(\text{M} - \text{Cl}_4)$		
$\nu_3 \nu(\text{M} - \text{Cl}')$		
$\nu_4 \pi(\text{MCl}_4)$		
$\nu_5 \nu(\text{M} - \text{Cl}_4)$		
$\nu_6 \pi(\text{MCl}_4)$		
$\nu_7 \delta(\text{ClMCl})$		
$\nu_8 \nu(\text{M} - \text{Cl}_4)$		
$\nu_9 \text{M} - \text{O} \text{ wag}$		
$\nu_{10} \delta(\text{ClMCl})$		
$\nu_{11} \text{M} - \text{Cl}' \text{ wag}$		

comparison with others of the series shows that the equivalent of the 180  $\text{cm}^{-1}$  band does often show a  $B_{3g}$  component. We are forced to conclude that the 276  $\text{cm}^{-1}$   $B_{3g}$  component is vanishingly weak.

Since  $B_{1g} + B_{3g}$  pairs can only derive from  $B_2$  and  $E$  modes in  $C_{4v}$  we have identified exactly the five required. In principle the single  $B_2$  mode [ $\delta(\text{ClMCl})$  in the ( $\text{FeCl}_4$ )

TABLE 12

Band count (internal modes only)

	$\text{Cs}[\text{InCl}_5 \cdot (\text{H}_2\text{O})]$	$\text{Cs}_2[\text{InCl}_5 \cdot (\text{D}_2\text{O})]$	$\text{K}_2[\text{FeCl}_5 \cdot (\text{H}_2\text{O})]$	$\text{K}_2[\text{FeCl}_5 \cdot (\text{D}_2\text{O})]$	$\text{Rb}_2[\text{FeCl}_5 \cdot (\text{H}_2\text{O})]$
$A_g$	7	7	7	5	5
$B_{1g}$	4	3	4	2	4
$B_{2g}$	2	1	1	1	1
$B_{3g}$	4	3	4	3	3

plane, and hence expected below 190  $\text{cm}^{-1}$ ] can be detected because, unlike the  $E$  modes, it should not have  $A_g$  and  $B_{2g}$  components. Thus far we have concluded that in terms of anion symmetry the five  $B_2 + E$  modes are at 276 ( $E$ ), 222 ( $E$ ), 180 ( $E$  or  $B_2$ ), 177/174 ( $E$  or  $B_2$ ) and 132/129  $\text{cm}^{-1}$  ( $E$  or  $B_2$ ). Being the highest of the  $E$  modes the 276  $\text{cm}^{-1}$  band is  $\nu_8$ ,  $\nu(\text{Fe}-\text{Cl})$ . It is equivalent to an  $E_u$  mode in a  $D_{4h}$  square-planar species (*i.e.*, Raman-inactive) and is only allowed in the present complexes by virtue of the relatively small distortion from  $D_{4h}$ . It was found to be extremely weak throughout the aquohalogeno-series and vanishingly weak in three of them.

On deuteration, the band at 384  $\text{cm}^{-1}$  is lowered by 13  $\text{cm}^{-1}$  and must be assigned as  $\nu(\text{Fe} \leftarrow \text{OH}_2)$ . The only other affected band is at 222  $\text{cm}^{-1}$ ; equivalent bands are seen to shift similarly in the indium salts and in the ammonium aquopentachloroferrates.  $\nu(\text{Fe} \leftarrow \text{OH}_2)$ ,  $\nu_1$ , and the  $\text{M}-\text{O}$  wag,  $\nu_9$ , are of  $A_1$  and  $E$  symmetry respectively.

The 132/129  $\text{cm}^{-1}$  pair are accompanied by an  $A_g$  band, and the 180  $\text{cm}^{-1}$   $B_{3g}$  band has an  $A_g$  component at 183

$\text{cm}^{-1}$ ; both therefore originate in  $E$  species. In contrast the 177/174  $\text{cm}^{-1}$  pair have no  $A_g$  component, as required for a  $B_2$  mode.

*A<sub>1</sub> and B<sub>1</sub> Modes.*—Both  $A_1$  and  $B_1$  modes should give  $A_g + B_{2g}$  doublets but we have only the  $A_g$  evidence in nearly all cases. In principle the relative intensities of the various derived tensor components should allow differentiation (Table 13) but in practice this has not occurred probably owing to inadequacy of the oriented gas model. Being deserted by group theory we have recourse to other

TABLE 13

Rotation of the polarisability tensor for  $\text{FeCl}_5(\text{H}_2\text{O})^{2-}$  by 45° about  $y$ 

	$C_{4v}$	$D_{2h}$
$A_1$	$\begin{bmatrix} a & 0 & 0 \\ 0 & a & 0 \\ 0 & 0 & b \end{bmatrix}$	$\begin{bmatrix} \frac{a+b}{2} & 0 & \frac{b-a}{2} \\ 0 & a & 0 \\ \frac{b-a}{2} & 0 & \frac{a+b}{2} \end{bmatrix}$
$B_1$	$\begin{bmatrix} c & 0 & 0 \\ 0 & -c & 0 \\ 0 & 0 & 0 \end{bmatrix}$	$\begin{bmatrix} \frac{1}{2}c & 0 & \frac{1}{2}c \\ 0 & -c & 0 \\ \frac{1}{2}c & 0 & \frac{1}{2}c \end{bmatrix}$
$B_2$	$\begin{bmatrix} 0 & d & 0 \\ d & 0 & 0 \\ 0 & 0 & 0 \end{bmatrix}$	$\begin{bmatrix} 0 & \sqrt{\frac{1}{2}}d & 0 \\ \sqrt{\frac{1}{2}}d & 0 & \sqrt{\frac{1}{2}}d \\ 0 & \frac{1}{2}\sqrt{d} & 0 \end{bmatrix}$
$E$	$\begin{bmatrix} 0 & 0 & 0 \\ 0 & 0 & e \\ 0 & e & 0 \end{bmatrix}$	$\begin{bmatrix} 0 & \sqrt{\frac{1}{2}}e & 0 \\ \sqrt{\frac{1}{2}}e & 0 & \sqrt{\frac{1}{2}}e \\ 0 & \sqrt{\frac{1}{2}}e & 0 \end{bmatrix}$
	$\begin{bmatrix} 0 & 0 & e \\ 0 & 0 & 0 \\ e & 0 & 0 \end{bmatrix}$	$\begin{bmatrix} -e & 0 & 0 \\ 0 & 0 & 0 \\ 0 & 0 & e \end{bmatrix}$

arguments. We note that  $\nu_2$ ,  $\nu_3$ , and  $\nu_5$  are all  $\nu(\text{Fe}-\text{Cl})$  modes and may reasonably be expected above 250  $\text{cm}^{-1}$ ; indeed  $\nu_8$ , the  $E$ -species  $\nu(\text{Fe}-\text{Cl})$  mode, has been located at 276  $\text{cm}^{-1}$ . Only one band, at 300  $\text{cm}^{-1}$ , was found in this region for the iron salts; therefore either  $\nu_2$ ,  $\nu_3$ , and  $\nu_5$  are coincident or one or more of these vibrations is vanishingly weak. One of the  $A_1$  modes is certainly likely to be weak. However, for the indates a second band is found (*i.e.*, 280 and 271  $\text{cm}^{-1}$ ). For the latter compound we place  $\nu_3$  below  $\nu_2$  in recognition of the greater length of the unique  $\text{In}-\text{Cl}$  bond compared with the other four. The possibility remains that the 271  $\text{cm}^{-1}$  band is the  $B_1$  mode and that the second  $A$  mode is missing.

It remains to locate the two  $\pi(\text{MCl}_4)$  modes,  $\nu_4(A_1)$  and  $\nu_6(B_1)$ . As only the 190 and 226  $\text{cm}^{-1}$  bands remain they are accordingly assigned jointly to these species. However, in a recent single-crystal study of the square-pyramidal  $[\text{InCl}_5]^{2-}$  the  $B_1 \pi(\text{MCl}_4)$  mode was found to be above the  $A_1$  mode.<sup>4</sup> We assume the same order for the aquo-complexes. The assignments are summarised in Table 10.

## DISCUSSION

Although there are four formula units in the unit cells of these crystals it has still proved feasible to discuss the spectra in terms of the full factor-group predictions so far as internal modes are concerned. We are now becoming familiar in Raman spectroscopy with the situation that some species tend to be vanishingly weak although formally allowed (the  $B_{2g}$  species in this case). Making allowance for this, we have seen

<sup>4</sup> D. M. Adams and R. R. Smardzewski, *J. Chem. Soc. (A)*, 1971, 714.

that the Raman results bear out factor-group predictions rather well. It remains to be seen whether the i.r. spectra fit this picture. Some molecular crystals having four molecules to the unit cell also show (even more clearly) the full factor-group splitting, although for tin

TABLE 14

Comparison of vibrational frequencies ( $\text{cm}^{-1}$ ) of  $[\text{InCl}_5]^{2-}$  and  $[\text{InCl}_5(\text{H}_2\text{O})]^{2-}$

	$[\text{InCl}_5]^{2-}$ <sup>a</sup>	$[\text{InCl}_5(\text{H}_2\text{O})]^{2-}$
$\nu(\text{In-Cl})$ {	$\nu_2(A_1)$ 294	280
	$\nu_3(A_1)$ 283	271
	$\nu_5(B_1)$ 287	280
	$\nu_8(E)$ 274	256
$\pi(\text{InCl}_4)$ {	$\nu_6(B_1)$ 193	215
	$\nu_4(B_1)$ 140	187
$\delta(\text{InCl}_4)$ {	$\nu_{10}(E)$ 143	162
	$\nu_7(B_2)$ 165	149
$\delta(\text{In-Cl})$	$\nu_{11}(E)$ 108	124

<sup>a</sup> Ref. 4.

tetraiodide with  $z = 8$  the limit seems to have been reached.<sup>5</sup>

In Table 14 we compare single-crystal assignments for  $(\text{Et}_4\text{N})_2[\text{InCl}_5]$ <sup>4</sup> and  $\text{Cs}_2[\text{InCl}_5(\text{H}_2\text{O})]$  as both have  $C_{4v}$  symmetry. The order of the stretching modes is similar in each case, with the  $E$  modes coming lowest,

and there is a general drop in  $\nu(\text{In-Cl})$  upon aquation. The X-ray data show that the  $\text{Cl}'\text{-In-Cl}$  angles,  $\theta$ , are  $103.9^\circ$  ( $[\text{InCl}_5]^{2-}$ ) and  $87.5^\circ$  ( $[\text{InCl}_5(\text{H}_2\text{O})]^{2-}$ ) respectively.  $\nu_8(E)$  will be *lowered* by increasing  $\theta$  owing to the form of the corresponding  $G$ -matrix element<sup>6</sup> but  $\nu_5(B_1)$  is independent of  $\theta$ ; we note that the difference in the  $\nu_5$  modes is the least of all the  $\nu(\text{In-Cl})$  modes. Since  $\nu_8$  is *raised* upon increasing  $\theta$  we conclude that the effect of decreasing the co-ordination number outweighs this effect, although it is possible that interaction with  $\nu_9(E)$  has some influence upon  $\nu_8$ .

Among the bending modes the  $B_1$  out-of-plane deformation is the highest in each case, and the lowest mode remains of  $E$  symmetry (probably the unique In-Cl wag). The most notable difference is the  $A_1$  out-of-plane bend which rises *ca.*  $50 \text{ cm}^{-1}$  upon aquation, probably owing to the relative ease with which this mode is executed in the absence of a sixth ligand.

We thank the S.R.C. for a grant (to D. C. N.) and for other support.

[1/1045 Received, 23rd June, 1971]

<sup>5</sup> D. M. Adams and W. S. Fernando, to be published.

<sup>6</sup> J. N. Murrell, *J. Chem. Soc. (A)*, 1969, 297.